

A Systematic Study of the Influence of Electrolyte Ions on the Electrode Activity

Xing Ding⁺,^[a] Daniel Scieszka⁺,^[a] Sebastian Watzele,^[a] Song Xue,^[a] Batyr Garlyyev,^[a] Richard W. Haid,^[a] and Aliaksandr S. Bandarenka^{*[a, b]}

Efficient electrocatalysis is most likely an answer to recent energy related challenges. Countless studies have been trying to find the links between the electrode/electrolyte interface structure, its composition, and the resulting activity in order to improve the performance of numerous devices, such as electrolyzers, fuel cells, and certain types of batteries. However, this scientific field currently meets serious complications associated with the prediction and explanation of an unexpected influence of seemingly inert electrolyte components on the observed

activity. Herein, we investigate various electrocatalytic systems using a unique laser-induced current transient technique to answer a long-lasting fundamental question: How can “inert” electrolytes change the activity so drastically? Different metal electrodes in contact with various aqueous solutions and two energy important reactions were used as model systems. We experimentally determine the potential of maximum entropy of the electrodes and find the connections between its position and the electrocatalytic performance.

Heterogeneous catalysis is of paramount importance in the synthesis of a vast majority of commodity products. In turn, electrocatalysis, being a part of heterogeneous catalysis, deals with reactions taking place at the so-called electrified interfaces formed between electron conductors (electrodes) and liquid electrolytes. Electrocatalysis currently plays one of the leading roles in overcoming problems related to sustainable energy provision and storage. While the catalytic performance of a certain electrode material depends on its structure and composition,^[1] there is also a strong and so far peculiar influence of the electrolyte composition on its activity.^[2] Today's electrocatalysis normally operates with a paradigm that there are only two major ways of increasing the rate of a catalytic reaction. The first one deals with the optimization of the electrode composition.^[3] The second one involves modifications of the electrode surface structure aiming to maximize the number of active sites.^[4] However, both approaches often exclude a very important part of the activity puzzle: electrolytes. In fact, the observed electrocatalyst performance is essentially a result of the influence of all these three major factors (Figure 1A).

The importance of the electrolyte composition for the resulting activity has been recognized decades ago,^[5] and there have been various research articles highlighting the electrolyte influence.^[6] However, there are not many systematic studies quantitatively showing the effects of the electrolyte species on the electrode/electrolyte interface structure. The reason behind this is related to fundamental methodological and theoretical difficulties: how, and particularly, what to measure and analyze, in order to explain the observed strong influence of the electrolyte components?


We start our discussion with the classical statement that electrocatalytic reactions should be intrinsically dependent on the properties of the electric double layer (EDL) formed between the electrodes and electrolytes.^[7] Therefore, a degree of order in the EDL influences the kinetics of electrocatalytic reactions.^[2a] In other words, the more ordered the interfacial layers are at a certain electrode potential, the more difficult for the EDL to rearrange itself after the electron transfer. If the structure and composition of the electrode surface are fixed, the net rate of the interfacial charge transfer should be maximal at the so-called potential of maximum entropy (PME) of the double layer formation (Figure 1B). Consequently, as shown in Figure 1C, one can anticipate that the closer the PME to the thermodynamic equilibrium potential of an electrocatalytic reaction is, the faster the respective reaction should be. This is schematically explained for the reactions important for sustainable energy provision, *i.e.*, the hydrogen evolution (HER, equilibrium potential: 0.00 V vs RHE) and the oxygen reduction (ORR, equilibrium potential: 1.23 V vs RHE) reactions, as illustrated in Figure 1C. In principle, one can arbitrarily consider this semi-quantitative consideration as an extrapolation of the conclusions of the Marcus's theory^[8] to the case of electrocatalytic processes.


One way to determine the PME experimentally is to use the laser-induced current transient (LICIT) technique (Figure 2).^[9] In this method, a short-time laser pulse of relatively low intensity

[a] Dr. X. Ding,⁺ Dr. D. Scieszka,⁺ Dr. S. Watzele, Dr. S. Xue, Dr. B. Garlyyev, R. W. Haid, Prof. Dr. A. S. Bandarenka
Physics of Energy Conversion and Storage
Technical University of Munich
James-Franck-Strasse 1, 85748 Garching, Germany
E-mail: bandarenka@ph.tum.de

[b] Prof. Dr. A. S. Bandarenka
Catalysis Research Center TUM
Technical University of Munich
Ernst-Otto-Fischer-Strasse 1, 85748 Garching, Germany

[†] These authors contributed equally to this work.

 Supporting information for this article is available on the WWW under <https://doi.org/10.1002/celec.202101088>

 © 2021 The Authors. ChemElectroChem published by Wiley-VCH GmbH. This is an open access article under the terms of the Creative Commons Attribution License, which permits use, distribution and reproduction in any medium, provided the original work is properly cited.

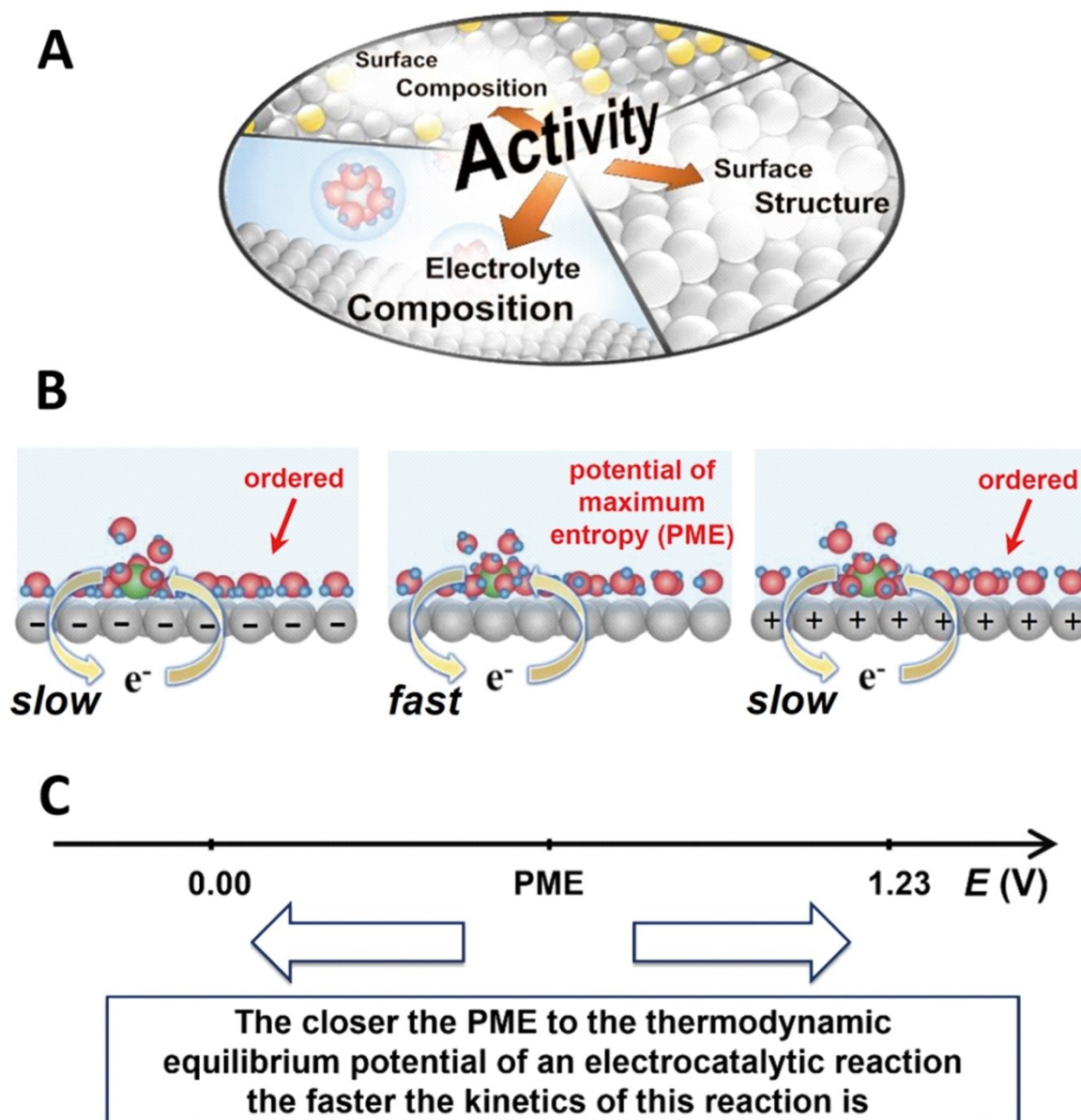


Figure 1. The electrocatalytic “activity puzzle”. (A) The catalytic performance of an electrode depends on its composition, structure, and the nature of the electrolyte species. (B) For a given electrode composition and structure, the rate of the interfacial electron transfer during a certain reaction should also depend on the degree of order in the electric double layer. (C) When a given electrode is in contact with various electrolytes, the reaction rate at the surface should be higher when the equilibrium potential for this reaction is closer to the potential of maximum entropy (PME) of the system. At this potential, the “energetic price” for the system reorganization after the electron transfer is the lowest.

hits the electrode surface under potential control and rapidly increases its temperature (by *ca* 30–40 K). This thermal probing “randomizes” ions and solvent molecules at the interface. Upon quick cooling of the system back to the initial temperature (and the initial EDL-state), relaxation of the current is monitored, as exemplified in Figure 3A. If the electrode surface at the controlled potential is charged negatively, the current spikes with the negative sign are observed. Conversely, the current peaks are positive if the surface is positively charged. In turn, at the PME the relaxation peaks are minimal, as the initial and final states are close to each other in sense of the interface order.

To test the aforementioned hypothesis about the fundamental connections between the position of the PME for a given catalytic system and its electrocatalytic performance, in this work, we performed a series of experiments involving different electrode materials in various electrolytes. As model reactions, the well-known hydrogen evolution and oxygen reduction reactions, which are important for renewable energy provision systems, were investigated. Let us consider these reactions taking place at different pHs (pH = 0; 0.5; 1.0; 1.5; and 2.0) on a polycrystalline platinum electrode (quartz crystal wafer), Pt_{pc} . To avoid the cation effect on the investigation of the pH effect, different concentrations of $HClO_4$ solutions are

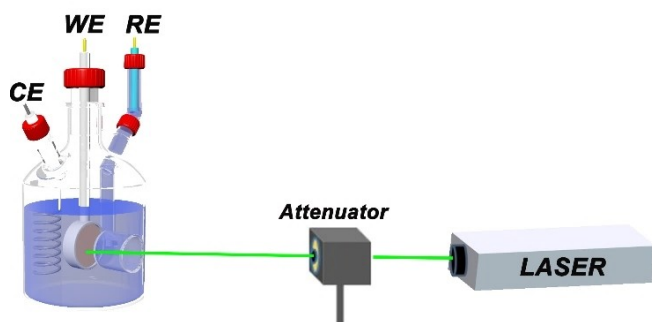


Figure 2. Schematic depiction of the LICT technique. WE, RE and CE correspond to working electrode, reference electrode and counter electrode, respectively.

utilized in this work. The model electrolytes in the initial LICT-experiments contained mainly protons (H^+), non-adsorbing ClO_4^- anions,^[10] and water molecules. Figure 3, B to E, shows that the PME values become more positive if the pH increases, which is in agreement with former studies of Pt electrodes.^[11] It should be noted that in these measurements the different pH values were achieved by adding the respective amount of HClO_4 and without balancing the ionic strength. The reason is that balancing the ionic strength requires adding alkali metal cations, which themselves affect the structure of the double layer, interfacial processes, and consequently the PME. Not balancing the ionic strength certainly has an impact on the electrolyte conductivity, however, this can be partially compensated by correcting the activity measurements for the high frequency electrolyte resistance, utilization of microelectrodes and by evaluation of activities at low current density. Furthermore, when comparing the CVs in Figure S2 one can see that the differences in conductivity are relatively small.

It is interesting that with the pH increase, the PME of the Pt electrodes shifts away from the thermodynamic equilibrium potential of the HER (0.00 V vs RHE) but closer to the equilibrium potential of the ORR (1.23 V vs RHE). Hence, according to the hypothesis, at higher pHs, those surfaces should demonstrate lower hydrogen evolution activity but at the same time higher activity towards the oxygen reduction in the same electrolytes. Indeed, the observed activities towards the respective reactions confirm the expected trend (see Figure 3, F and G).

Interestingly, similar trends were observed for a polycrystalline Au-electrode (quartz crystal wafer, Au_{pc}). As depicted in Figure 3H, the PME for the Au_{pc} electrocatalyst shifts to more positive potentials upon the pH increase. Sample current transients obtained for Au_{pc} electrodes are shown in Figure S1. In addition, note that the reconstruction of the gold surface could also contribute to the shift of the PME.^[12] As in the case of the Pt_{pc} electrodes, in the electrolytes with high H^+ concentrations, their activity towards the hydrogen evolution increases (Figure 3I). On the contrary, a decrease in the H^+ concentration results in faster oxygen reduction kinetics (Figure 3J).

Besides, typical cyclic voltammograms (CVs) for AT-cut Pt and Au quartz crystal wafers were recorded in HClO_4 solutions

of various pH values before and after the laser measurements (see Figure S2 and S3). The CVs did not change after the laser measurements for both Pt and Au, confirming that the irradiation is not altering the surface quality.

The analysis of the simple systems presented above motivates to find the origin of the electrolyte-related dependencies with respect to the electrode activity. Therefore, we performed PME-measurements using the polycrystalline platinum electrode in electrolytes containing alkali metal cations. Near-to-neutral pH (pH = 6) solutions of 0.5 M Li_2SO_4 , Na_2SO_4 , K_2SO_4 , and Cs_2SO_4 were chosen to maximally reduce the influence of the H^+ and OH^- ions on the system without losing the ability to control their concentration. In turn, by replacing the ClO_4^- anions with the SO_4^{2-} (characterized by high hydration energy) it was possible to avoid competition between the effects shown by cations and anions present in the electrolytes.^[13] Besides, comparing the CVs for Pt_{pc} in the electrolytes containing Li^+ and Cs^+ (Figure S4), one can see that hydrogen adsorption processes were particularly not affected by cations. This was also observed for the case of $\text{Pt}(111)$.^[2g]

As presented in Figure 4, A to D, the PME values of the Pt_{pc} electrodes are ~ 0.11 , ~ 0.18 , ~ 0.22 , and ~ 0.25 V in the presence of Li^+ , Na^+ , K^+ , and Cs^+ , respectively. The plot of the PME values against the hydration energy of the alkali metal cation reveals a linear relationship (Figure 4E). In line with the above-described hypothesis, the rate of the hydrogen evolution increases in the Li^+ -containing solutions (Figure 4F), while the activity towards the oxygen reduction gets higher in the presence of Cs^+ (Figure 4G). Interestingly, the PME of the Au_{pc} surface shows the same trends in the neutral pH (pH ~ 7) solutions of 0.25 M Na_2SO_4 and K_2SO_4 (Figure 4H). Sample current transients obtained for Au_{pc} electrodes in the near-to-neutral electrolytes are shown in Figure S5. Note, the larger difference of the PME can be also due to 2D surface phase transitions in the adsorbate layers in the presence of K^+ .^[15] The measured activity of the Au_{pc} surface towards the hydrogen evolution is higher in the presence of Na^+ (Figure 4I), whereas the oxygen reduction activity is higher in the K^+ -containing electrolyte (Figure 4J) – all in accordance with the PME-changes.

Figure 5 summarizes correlations between the observed electrode activities and the PME. As shown in Figure 5, A and E, the activity of both the Pt_{pc} and Au_{pc} towards the hydrogen evolution (expressed as the exchange current density, j_0) in solutions of various pHs decreases linearly with the PME increase. In the case of the hydrogen evolution activities of Pt_{pc} in electrolytes containing alkali metal cations, the potential (vs RHE) at a current density of -5 mA cm^{-2} increases linearly with the PME moving away from the HER equilibrium potential (Figure 5C). In turn, as depicted in Figure 5, B and D, the oxygen reduction activities of the Pt electrodes, quantified in terms of the half-wave potentials, $E_{1/2}$, rises with the PME. Figure 5F additionally compares the activity trend of the Pt_{pc} surface towards the oxygen reduction presented in Figure 5, B and D. Interestingly, both trends exhibit a similar slope.

The examples presented above show that the resulting electrocatalytic activity of investigated systems depends on the

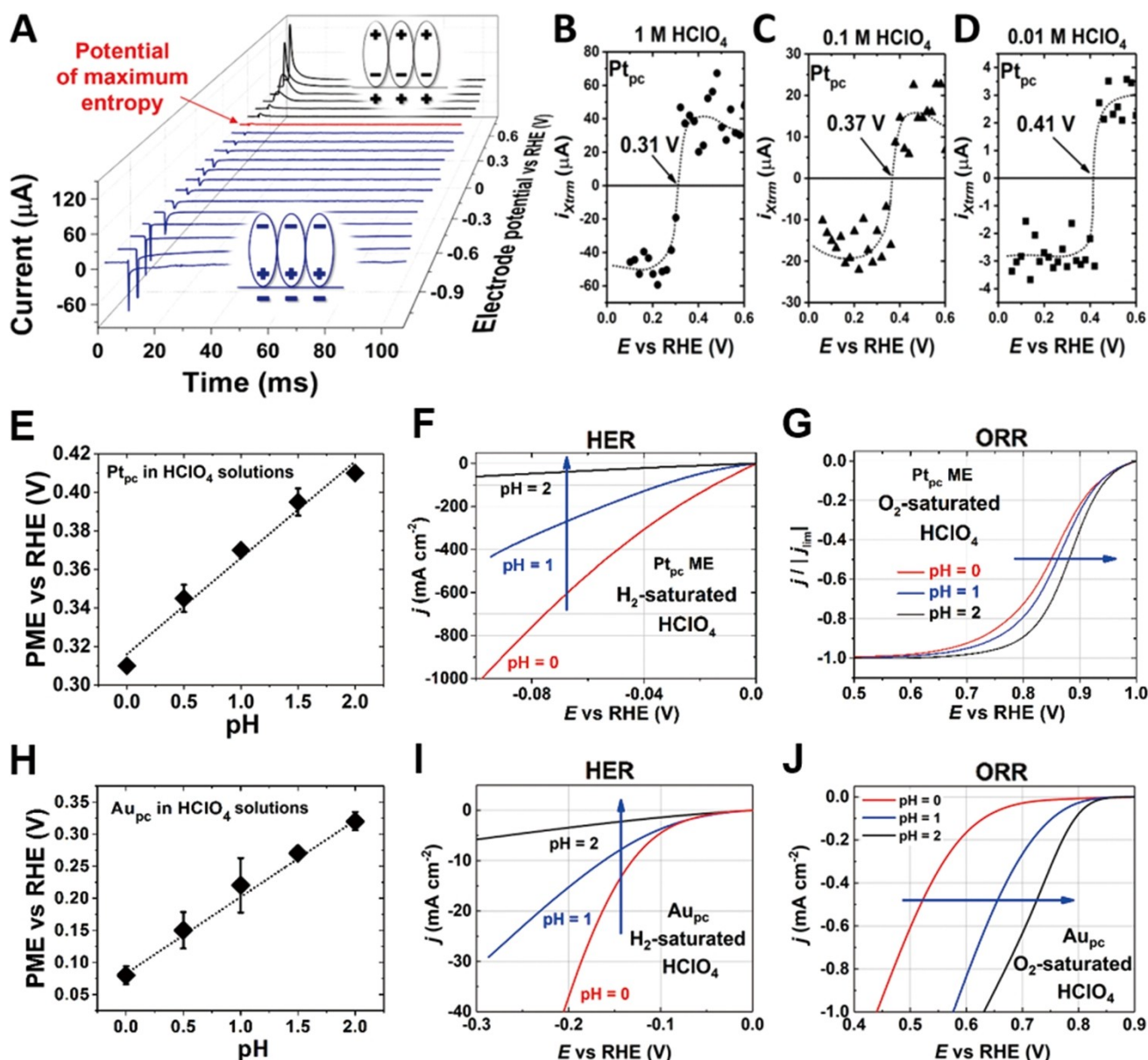


Figure 3. The positions of the potential of maximum entropy (PME) and activities towards hydrogen evolution and oxygen reduction reactions. (A) An example of the relaxation peaks obtained for Au-electrode by the laser-induced current transient technique used to find the PME. (B to D) The values of the current spikes maxima (i_{xtrm}) as a function of pH for the Pt-electrodes in different electrolytes as indicated in the figures. These plots enable to identify the location of the PME. Splined lines serve as guidance for the eye. (E) The PME of Pt_{pc} electrodes shifts towards more positive values as a result of the pH increase. Consequently, within the presented model, (F) the activity of Pt_{pc} microelectrode (depicted as Pt_{pc} ME) decreases towards the hydrogen evolution reaction and (G) increases towards the oxygen reduction reaction (The obtained currents have been normalized to the limiting current density (j_{lim}) for easier comparison) upon the pH increase (traced with arrows). (H) The PME of the Au_{pc} electrode as a function of the electrolyte pH. One can observe an analogous increase in the PME as a consequence of the pH rise. Note that, as in the previous case, increase in the pH results in (I) the loss in the electrode activity towards hydrogen evolution and (J) the enhancement of its activity towards oxygen reduction (Note that, for better visibility, only the ORR kinetics dominated region is shown). Details of the activity measurements can be found in the Supporting Information. Error bars represent SD.

electrochemical interface order. In the investigated solutions, the influence of the electrolyte species (their nature and concentration) on the interface behavior can be predictable. Let us attempt to describe the observed effect quantitatively. The degree of order at the electrode/electrolyte interface is associated with the “collective” polarizability of the electrolyte which, in turn, can be quantified by the relative dielectric constant, ϵ_r .^[2c,16] This parameter depends on the concentration

and the nature of the electrolyte species. In solutions characterized by a concentration lower than 2 M, ϵ_r demonstrates changes with the electrolyte concentration,^[16] as described by the following general equation:

$$\epsilon_r = \epsilon_{pure\ H_2O} - \alpha(C_{ion}) \quad (1)$$

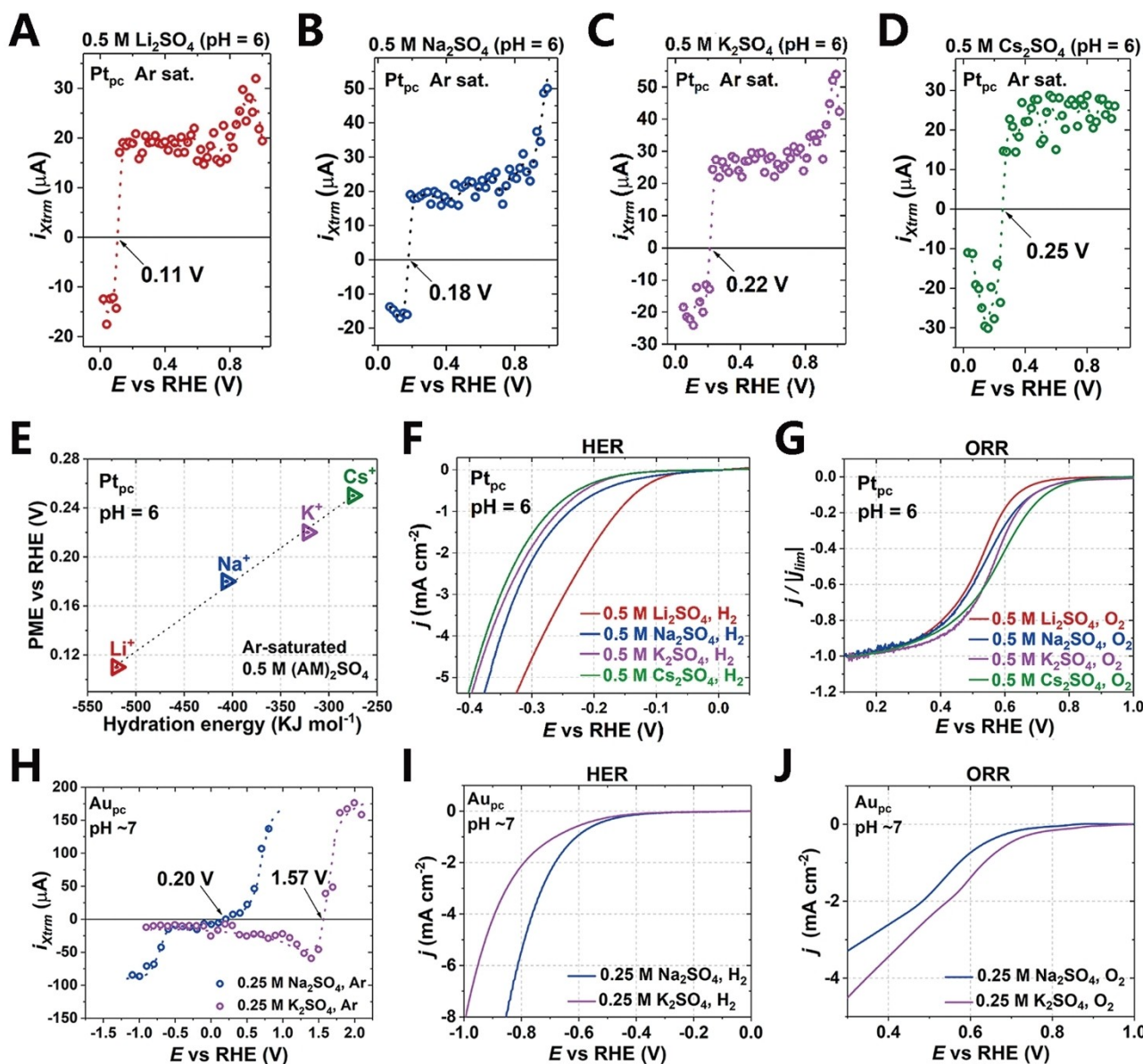


Figure 4. Hydrogen evolution and oxygen reduction activities of the polycrystalline Pt and Au electrodes correlated with the corresponding PME values measured in electrolytes containing alkali metal cations. (A to D) Determination of the PME for Pt_{pc} electrodes in electrolytes containing alkali metal cations. The PME largely depends on the nature of the alkali-metal cations, which can be further confirmed by (E) the correlation between the PME and the hydration energies of the alkali metal cations (AM = Li⁺, Na⁺, K⁺, Cs⁺). The change in the PME influences the rate of the electrochemical processes. Hence, (F) the Pt_{pc} activity towards hydrogen evolution is higher in the presence of Li⁺, whereas (G) the oxygen reduction activity is higher in the presence of Cs⁺ (The obtained currents have been normalized to the limiting current density (j_{lim}) for easier comparison). As shown in ref. [14], the negative current offset shift in (F) results from the alteration in the pH near the electrode surface. (H) Analogous plot showing the PME values of the Au_{pc} electrode in solutions of sodium and potassium salts. As for Pt_{pc}, (I) the rate of hydrogen evolution on Au_{pc} is higher in the Na⁺-containing electrolyte, while (J) the oxygen reduction rate is higher in the presence of K⁺ cations.

where $\epsilon_{pure\ H_2O}$ stands for the dielectric constant of pure water ($\epsilon_{pure\ H_2O} \sim 82$ at room temperature), the function α describes the relative ion contribution, and C_{ion} is the ion concentration.^[16] It should be noted that in most systems at higher concentrations, ϵ_r demonstrates a quasi-linear behavior. As shown in Figure 3, E and H, as well as in previous reports,^[17] within a narrow concentration range, a linear trend is observed for the PME. Thus, one can assume the following general formal expression for the potential of maximum entropy, E_{PME} :

$$E_{PME} = E_{PME}^{at\ \epsilon = \epsilon_{pure\ H_2O}} \pm \beta(C_{ion}) \quad (2)$$

where $E_{PME}^{at\ \epsilon = \epsilon_{pure\ H_2O}}$ stands for the E_{PME} value assumed for a hypothetical system containing only pure water, while the function β describes the relative contribution of the ion concentration.

Since the activity towards certain reactions within the investigated concentration regimes changes linearly with the PME value, also in this case, the electrode activity can be described with the general formula of the linear function.

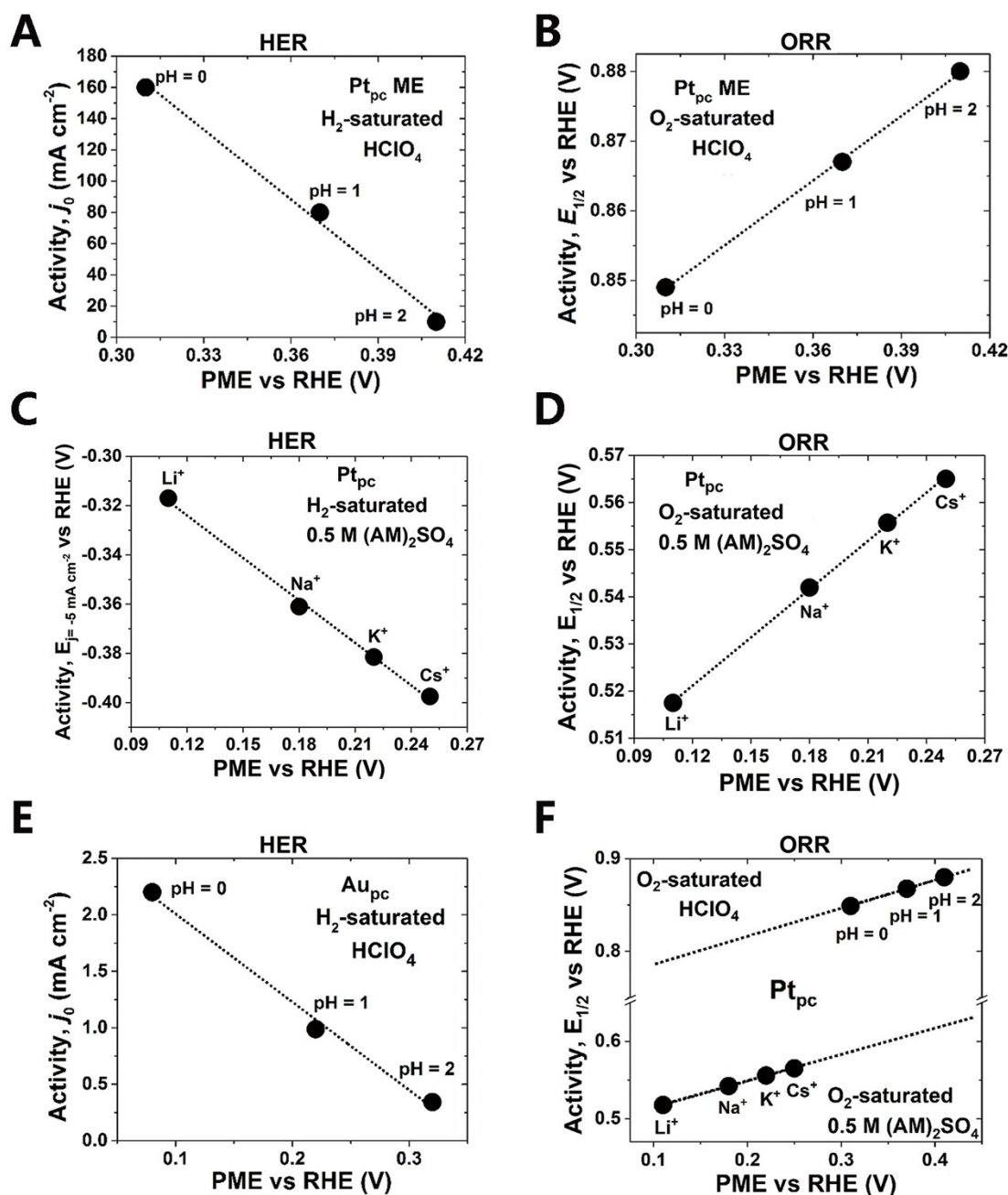


Figure 5. Correlations between the electrocatalytic activity and the corresponding PMEs. (A) Pt_{pc} microelectrode (depicted as Pt_{pc} ME) activities towards the hydrogen evolution expressed as the exchange current density, j_0 and (B) the oxygen reduction activity expressed as the half-wave potential, $E_{1/2}$, in the HClO_4 solutions of various pHs as a function of the PME. (C) Pt_{pc} activities towards the hydrogen evolution expressed as the potential (vs RHE) required for a current density of -5 mA cm^{-2} and (D) the oxygen reduction activity expressed as $E_{1/2}$ in the electrolytes containing $0.5 \text{ M (AM)}_2\text{SO}_4$ ($\text{AM} = \text{Li}^+, \text{Na}^+, \text{K}^+, \text{Cs}^+$) as a function of the PME. (E) Hydrogen evolution activities of Au_{pc} electrode expressed as the exchange current density j_0 in solutions of various pHs as a function of the PME. Although, the obtained trends for the hydrogen evolution and oxygen reduction reactions are opposite to each other, the electrocatalytic activities change linearly with the PME values. (F) Comparison of the $E_{1/2}$ vs PME dependencies obtained for the Pt_{pc} electrode, both in the HClO_4 solutions and $0.5 \text{ M (AM)}_2\text{SO}_4$ ($\text{AM} = \text{Li}^+, \text{Na}^+, \text{K}^+, \text{Cs}^+$). Note the similar slopes of the activity trend lines in both groups of electrolytes.

Furthermore, by rearranging eq. 1 in terms of C_{ion} and combining it with eq. 2, one can express the PME value as a function of the dielectric constant. Thus, taking the electrode activity in pure water, $A_{\text{H}_2\text{O}}$, as the reference, the formula for the electrode activity, A , can be expressed as follows:

$$A \propto A_{\text{H}_2\text{O}} \pm \tilde{\varphi} [\varepsilon_{\text{pure H}_2\text{O}} - \varepsilon_r^{\text{electrolyte}}] \quad (3)$$

where $\tilde{\varphi}$ is a function, which is most likely dependent on the nature of the reaction.

In summary, a systematic study of the influence of the interfacial properties on the electrode activity was presented. A unique LICt technique was used to successfully measure the

PME of the electrodes in contact with various complex solutions. Observations herein disclose the critical importance of the electrolyte composition for the performance of electrocatalytic systems. The presented qualitative and quantitative explanations of the observed effects clarify their origins and systematize new and existing knowledge about the role of electrolyte species. The presented approaches can be promptly applied to describe the activity of other mono- and polycyclic electrodes submerged in aqueous electrolytes. Hence, these studies open up a new avenue in heterogeneous catalysis enabling to model and understand the electrocatalytic behavior of various systems.

Acknowledgements

The financial support from Deutsche Forschungsgemeinschaft (DFG) under Germany's excellence strategy – EXC 2089/1-390776260, Germany's excellence cluster “e-conversion”, DFG projects BA 5795/6-1, BA 5795/5-1 and BA 5795/4-1, and funding from the TUM IGSSSE project 11.01 are gratefully acknowledged. X.D. and S.X. are thankful for the financial support from the China Scholarship Council. Open Access funding enabled and organized by Projekt DEAL.

Conflict of Interest

The authors declare no conflict of interest.

Keywords: Electric double layer · Electrocatalysis · Electrolyte influence · Laser-induced current transient · Potential of maximum entropy

- [1] a) J. Greeley, I.E.L. Stephens, A.S. Bondarenko, T.P. Johansson, H.A. Hansen, T.F. Jaramillo, J. Rossmeisl, I. Chorkendorff, *Nat. Chem.* **2009**, *1*, 552–556; b) F. Calle-Vallejo, J. Tymoczko, V. Colic, Q.H. Vu, M.D. Pohl, K. Morgenstern, D. Loffreda, P. Sautet, W. Schuhmann, A.S. Bandarenka, *Science* **2015**, *350*, 185–189; c) J.H.K. Pfisterer, Y. Liang, O. Schneider, A.S. Bandarenka, *Nature* **2017**, *549*, 74–77; d) Z.W. Seh, J. Kibsgaard, C.F. Dickens, I. Chorkendorff, J.K. Nørskov, T.F. Jaramillo, *Science* **2017**, *355*, eaad4998, doi: 10.1126/science.aad4998; e) M. Rück, B. Garlyyev, F. Mayr, A.S. Bandarenka, A. Gagliardi, *J. Phys. Chem. Lett.* **2020**, *11*, 1773–1780; f) J. Fichtner, B. Garlyyev, S. Watzel, H.A. El-Sayed, J. Schwaemmlein, W. Li, F. Maillard, L. Dubau, J. Michalicka, J. Macak, A.W. Holleitner, A.S. Bandarenka, *ACS Appl. Mater. Interfaces* **2019**, *11*, 5129–5135; g) F. Faisal, C. Stumm, M. Bertram, F. Waidhas, Y. Lykhach, S. Cherevko, F. Xiang, M. Ammon, M. Vorokhta, B. Šmid, *Nat. Mater.* **2018**, *17*, 592–598.
- [2] a) I. Ledezma-Yanez, W.D.Z. Wallace, P. Sebastián-Pascual, V. Climent, J.M. Feliu, M.T.M. Koper, *Nat. Energy* **2017**, *2*, 17031; b) C. Stoffelsma, P. Rodriguez, G. Garcia, N. Garcia-Araez, D. Strmcnik, N.M. Markovic, M.T.M. Koper, *J. Am. Chem. Soc.* **2010**, *132*, 16127–16133; c) S. Xue, R.W. Haid, R.M. Kluge, X. Ding, B. Garlyyev, J. Fichtner, S. Watzel, S. Hou, A.S. Bandarenka, *Angew. Chem. Int. Ed.* **2020**, *59*, 10934–10938; *Angew. Chem.* **2020**, *132*, 11026–11031; d) B. Garlyyev, S. Xue, S. Watzel, D. Scieszka, A.S. Bandarenka, *J. Phys. Chem. Lett.* **2018**, *9*, 1927–1930; e) R. Rizo, E. Herrero, J.M. Feliu, *Phys. Chem. Chem. Phys.* **2013**, *15*, 15416–15425; f) Y. Liang, D. Mclaughlin, C. Csoklich, O. Schneider, A.S. Bandarenka, *Energy Environ. Sci.* **2019**, *12*, 351–357; g) D. Strmcnik, K. Kodama, D. Van der Vliet, J. Greeley, V.R. Stamenkovic, N.M. Markovic, *Nat. Chem.* **2009**, *1*, 466–472; h) S. Xue, B. Garlyyev, A. Auer, J. Kunze-Liebhäuser, A.S. Bandarenka, *J. Phys. Chem. C* **2020**, *124*, 12442–12447; i) B. Garlyyev, S. Xue, M.D. Pohl, D. Reinisch, A.S. Bandarenka, *ACS Omega* **2018**, *3*, 15325–15331; j) D. Gao, R.M. Arán-Ais, H.S. Jeon, B.R. Cuenya, *Nat. Catal.* **2019**, *2*, 198–210; k) M.R. Singh, Y. Kwon, Y. Lum, J.W. Ager III, A.T. Bell, *J. Am. Chem. Soc.* **2016**, *138*, 13006–13012; l) Z. Yang, Q. Li, K.C. Chou, *J. Phys. Chem. C* **2009**, *113*, 8201–8205; m) X. Chen, I.T. McCrum, K.A. Schwarz, M.J. Janik, M.T. Koper, *Angew. Chem. Int. Ed.* **2017**, *56*, 15025–15029; *Angew. Chem.* **2017**, *129*, 15221–15225.
- [3] a) A.S. Bandarenka, M.T.M. Koper, *J. Catal.* **2013**, *308*, 11–24; b) X. Tian, X. Zhao, Y.Q. Su, L. Wang, H. Wang, D. Dang, B. Chi, H. Liu, E.J.M. Hensen, X.W.D. Lou, B.Y. Xia, *Science* **2019**, *366*, 850–856; c) H. Wang, L. Wang, Q. Wang, S. Ye, W. Sun, Y. Shao, Z. Jiang, Q. Qiao, Y. Zhu, P. Song, *Angew. Chem. Int. Ed.* **2018**, *57*, 12360–12364; *Angew. Chem.* **2018**, *130*, 12540–15544; d) J. Wang, H. Zhu, D. Yu, J. Chen, J. Chen, M. Zhang, L. Wang, M. Du, *ACS Appl. Mater. Interfaces* **2017**, *9*, 19756–19765; e) S.A. Mauger, K. Neyerlin, S.M. Alia, C. Ngo, S.K. Babu, K.E. Hurst, S. Pylypenko, S. Litster, B.S. Pivovar, *J. Electrochem. Soc.* **2018**, *165*, F238.
- [4] a) B. Garlyyev, J. Fichtner, O. Piqué, O. Schneider, A.S. Bandarenka, F. Calle-Vallejo, *Chem. Sci.* **2019**, *10*, 8060–8075; b) B. Garlyyev, K. Kratzl, M. Rück, J. Michalicka, J. Fichtner, J. Macak, T. Kratky, S. Günther, M. Cokoja, A.S. Bandarenka, A. Gagliardi, R.A. Fischer, *Angew. Chem. Int. Ed.* **2019**, *58*, 9596–9600; *Angew. Chem.* **2019**, *58*, 9596–9600; c) E. Pomerantseva, F. Bonaccorso, X. Feng, Y. Cui, Y. Gogotsi, *Science* **2019**, *366*, eaan8285; d) J. Hou, M. Yang, C. Ke, G. Wei, C. Priest, Z. Qiao, G. Wu, J. Zhang, *EnergyChem* **2020**, *2*, 100023; e) W.-R. Liu, Z.-Z. Guo, W.-S. Young, D.-T. Shieh, H.-C. Wu, M.-H. Yang, N.-L. Wu, *J. Power Sources* **2005**, *140*, 139–144.
- [5] a) P. Herasymenko, I. Slendyk, *Z. Phys. Chem. Abt. A* **1930**, *149*, 123; b) M. Tokuoaka, *Collect. Czech. Chem. Commun.* **1932**, *4*, 444–455; c) A.N. Frumkin, *Trans. Faraday Soc.* **1959**, *55*, 156–167.
- [6] a) Y.Y. Birdja, E. Pérez-Gallent, M.C. Figueiredo, A.J. Göttle, F. Calle-Vallejo, M.T. Koper, *Nat. Energy* **2019**, *4*, 732–745; b) J.A. Lopez-Ruiz, U. Sanyal, J. Egbert, O.Y. Gutiérrez, J. Holladay, *ACS Sustainable Chem. Eng.* **2018**, *6*, 16073–16085; c) T. Shinagawa, K. Takanabe, *ChemSusChem* **2017**, *10*, 1318; d) E. Pérez-Gallent, G. Marcandalli, M.C. Figueiredo, F. Calle-Vallejo, M.T. Koper, *J. Am. Chem. Soc.* **2017**, *139*, 16412–16419; e) D. Bohra, J.H. Chaudhry, T. Burdyny, E.A. Pidko, W.A. Smith, *Energy Environ. Sci.* **2019**, *12*, 3380–3389.
- [7] a) M. Breiter, M. Kleinerman, P. Delahay, *J. Am. Chem. Soc.* **1958**, *80*, 5111–5117; b) A.N. Frumkin, *J. Electrochem. Soc.* **1960**, *107*, 461–472.
- [8] R.A. Marcus, *Ann. Rev. Phys. Chem.* **1964**, *15*, 155–196.
- [9] a) V.A. Benderskii, S.D. Babenko, A.G. Krivenko, *J. Electroanal. Chem. Interfacial Electrochem.* **1978**, *86*, 223–225; b) V. Climent, B.A. Coles, R.G. Compton, *J. Phys. Chem. B* **2001**, *105*, 10669–10673; c) D. Scieszka, J. Yun, A.S. Bandarenka, *ACS Appl. Mater. Interfaces* **2017**, *9*, 20213–20222; d) A. Auer, X. Ding, A.S. Bandarenka, J. Kunze-Liebhäuser, *J. Phys. Chem. C* **2021**, *125*, 5020–5028.
- [10] M.D. Pohl, V. Colic, D. Scieszka, A.S. Bandarenka, *Phys. Chem. Chem. Phys.* **2016**, *18*, 10792–10799.
- [11] N. Garcia-Araez, V. Climent, J.M. Feliu, *J. Phys. Chem. C* **2009**, *113*, 9290–9304.
- [12] V. Climent, B.A. Coles, R.G. Compton, *J. Phys. Chem. B* **2002**, *106*, 5258–5265.
- [13] D.W. Smith, *J. Chem. Educ.* **1977**, *54*, 540–542.
- [14] M. Auinger, I. Katsounaros, J.C. Meier, S.O. Klemm, P.U. Biedemann, A.A. Topalov, M. Rohwerder, K.J.J. Mayrhofer, *Phys. Chem. Chem. Phys.* **2011**, *13*, 16384–16394.
- [15] X. Ding, B. Garlyyev, S.A. Watzel, T.K. Sarpey, A.S. Bandarenka, *Chem. Eur. J.* **2021**, *27*, 10016–10020.
- [16] J.B. Hasted, D.M. Ritson, C.H. Collie, *J. Chem. Phys.* **1948**, *16*, 1–21.
- [17] A. Ganassin, P. Sebastian, V. Climent, W. Schumann, A.S. Bandarenka, J.M. Feliu, *Sci. Rep.* **2017**, *7*, 1243.

Manuscript received: August 8, 2021

Revised manuscript received: November 19, 2021

Accepted manuscript online: November 22, 2021